Top quark mass measurement using the template method at CDF

T. Aaltonen *et al.* (CDF Collaboration)

Top quark mass measurement using the template method at CDF

T. Aaltonen,[21] B. Álvarez González[v],[9] S. Amerio,[41] D. Amidei,[32] A. Anastassov,[36] A. Annovi,[17] J. Antos,[12] G. Apollinari,[15] J.A. Appel,[15] A. Apresyan,[46] T. Arisawa,[56] A. Artikov,[13] J. Asaadi,[51] W. Ashmanskas,[15] B. Auerbach,[59] A. Aurisano,[51] F. Azfar,[40] W. Badgett,[15] A. Barbaro-Galtieri,[26] V.E. Barnes,[46] B.A. Barnett,[23] P. Barria[cc],[44] P. Bartos,[12] M. Bauce[aa],[41] G. Bauer,[30] F. Bedeschi,[44] D. Beecher,[28] S. Behari,[23] G. Bellettini[bb],[44] J. Bellinger,[58] D. Benjamin,[14] A. Beretvas,[15] A. Bhatti,[48] M. Binkley[*],[15] D. Bisello[aa],[41] I. Bizjak[gg],[28] K.R. Bland,[5] B. Blumenfeld,[23] A. Bocci,[14] A. Bodek,[47] D. Bortoletto,[46] J. Boudreau,[45] A. Boveia,[11] B. Brau[a],[15] L. Brigliadori[z],[6] A. Brisuda,[12] C. Bromberg,[33] E. Brucken,[21] M. Bucciantonio[bb],[44] J. Budagov,[13] H.S. Budd,[47] S. Budd,[22] K. Burkett,[15] G. Busetto[aa],[41] P. Bussey,[19] A. Buzatu,[31] C. Calancha,[29] S. Camarda,[4] M. Campanelli,[33] M. Campbell,[32] F. Canelli[12],[15] A. Canepa,[43] B. Carls,[22] D. Carlsmith,[58] R. Carosi,[44] S. Carrillo[k],[16] S. Carron,[15] B. Casal,[9] M. Casarsa,[15] A. Castro[z],[6] P. Catastini,[15] D. Cauz,[52] V. Cavaliere[cc],[44] M. Cavalli-Sforza,[4] A. Cerri[f],[26] L. Cerrito[q],[28] Y.C. Chen,[1] M. Chertok,[7] G. Chiarelli,[44] G. Chlachidze,[15] F. Chlebana,[15] K. Cho,[25] D. Chokheli,[13] J.P. Chou,[20] W.H. Chung,[58] Y.S. Chung,[47] C.I. Ciobanu,[42] M.A. Ciocci[cc],[44] A. Clark,[18] G. Compostella[aa],[41] M.E. Convery,[15] J. Conway,[7] M.Corbo,[42] M. Cordelli,[17] C.A. Cox,[7] D.J. Cox,[7] F. Crescioli[bb],[44] C. Cuenca Almenar,[59] J. Cuevas[v],[9] R. Culbertson,[15] D. Dagenhart,[15] N. d'Ascenzo[t],[42] M. Datta,[15] P. de Barbaro,[47] S. De Cecco,[49] G. De Lorenzo,[4] M. Dell'Orso[bb],[44] C. Deluca,[4] L. Demortier,[48] J. Deng[c],[14] M. Deninno,[6] F. Devoto,[21] M. d'Errico[aa],[41] A. Di Canto[bb],[44] B. Di Ruzza,[44] J.R. Dittmann,[5] M. D'Onofrio,[27] S. Donati[bb],[44] P. Dong,[15] M. Dorigo,[52] T. Dorigo,[41] K. Ebina,[56] A. Elagin,[51] A. Eppig,[32] R. Erbacher,[7] D. Errede,[22] S. Errede,[22] N. Ershaidat[y],[42] R. Eusebi,[51] H.C. Fang,[26] S. Farrington,[40] M. Feindt,[24] J.P. Fernandez,[29] C. Ferrazza[dd],[44] R. Field,[16] G. Flanagan[r],[46] R. Forrest,[7] M.J. Frank,[5] M. Franklin,[20] J.C. Freeman,[15] Y. Funakoshi,[56] I. Furic,[16] M. Gallinaro,[48] J. Galyardt,[10] J.E. Garcia,[18] A.F. Garfinkel,[46] P. Garosi[cc],[44] H. Gerberich,[22] E. Gerchtein,[15] S. Giagu[ee],[49] V. Giakoumopoulou,[3] P. Giannetti,[44] K. Gibson,[45] C.M. Ginsburg,[15] N. Giokaris,[3] P. Giromini,[17] M. Giunta,[44] G. Giurgiu,[23] V. Glagolev,[13] D. Glenzinski,[15] M. Gold,[35] D. Goldin,[51] N. Goldschmidt,[16] A. Golossanov,[15] G. Gomez,[9] G. Gomez-Ceballos,[30] M. Goncharov,[30] O. González,[29] I. Gorelov,[35] A.T. Goshaw,[14] K. Goulianos,[48] A. Gresele,[41] S. Grinstein,[4] C. Grosso-Pilcher,[11] R.C. Group,[55] J. Guimaraes da Costa,[20] Z. Gunay-Unalan,[33] C. Haber,[26] S.R. Hahn,[15] E. Halkiadakis,[50] A. Hamaguchi,[39] J.Y. Han,[47] F. Happacher,[17] K. Hara,[53] D. Hare,[50] M. Hare,[54] R.F. Harr,[57] K. Hatakeyama,[5] C. Hays,[40] M. Heck,[24] J. Heinrich,[43] M. Herndon,[58] S. Hewamanage,[5] D. Hidas,[50] A. Hocker,[15] W. Hopkins[g],[15] D. Horn,[24] S. Hou,[1] R.E. Hughes,[37] M. Hurwitz,[11] U. Husemann,[59] N. Hussain,[31] M. Hussein,[33] J. Huston,[33] G. Introzzi,[44] M. Iori[ee],[49] A. Ivanov[o],[7] E. James,[15] D. Jang,[10] B. Jayatilaka,[14] E.J. Jeon,[25] M.K. Jha,[6] S. Jindariani,[15] W. Johnson,[7] M. Jones,[46] K.K. Joo,[25] S.Y. Jun,[10] T.R. Junk,[15] T. Kamon,[51] P.E. Karchin,[57] Y. Kato[n],[39] W. Ketchum,[11] J. Keung,[43] V. Khotilovich,[51] B. Kilminster,[15] D.H. Kim,[25] H.S. Kim,[25] H.W. Kim,[25] J.E. Kim,[25] M.J. Kim,[17] S.B. Kim,[25] S.H. Kim,[53] Y.K. Kim,[11] N. Kimura,[56] M. Kirby,[15] S. Klimenko,[16] K. Kondo,[56] D.J. Kong,[25] J. Konigsberg,[16] A.V. Kotwal,[14] M. Kreps,[24] J. Kroll,[43] D. Krop,[11] N. Krumnack[l],[5] M. Kruse,[14] V. Krutelyov[d],[51] T. Kuhr,[24] M. Kurata,[53] S. Kwang,[11] A.T. Laasanen,[46] S. Lami,[44] S. Lammel,[15] M. Lancaster,[28] R.L. Lander,[7] K. Lannon[u],[37] A. Lath,[50] G. Latino[cc],[44] I. Lazzizzera,[41] T. LeCompte,[2] E. Lee,[51] H.S. Lee,[11] J.S. Lee,[25] S.W. Lee[w],[51] S. Leo[bb],[44] S. Leone,[44] J.D. Lewis,[15] C.-J. Lin,[26] J. Linacre,[40] M. Lindgren,[15] E. Lipeles,[43] A. Lister,[18] D.O. Litvintsev,[15] C. Liu,[45] Q. Liu,[46] T. Liu,[15] S. Lockwitz,[59] N.S. Lockyer,[43] A. Loginov,[59] D. Lucchesi[aa],[41] J. Lueck,[24] P. Lujan,[26] P. Lukens,[15] G. Lungu,[48] J. Lys,[26] R. Lysak,[12] R. Madrak,[15] K. Maeshima,[15] K. Makhoul,[30] P. Maksimovic,[23] S. Malik,[48] G. Manca[b],[27] A. Manousakis-Katsikakis,[3] F. Margaroli,[46] C. Marino,[24] M. Martínez,[4] R. Martínez-Ballarín,[29] P. Mastrandrea,[49] M. Mathis,[23] M.E. Mattson,[57] P. Mazzanti,[6] K.S. McFarland,[47] P. McIntyre,[51] R. McNulty[i],[27] A. Mehta,[27] P. Mehtala,[21] A. Menzione,[44] C. Mesropian,[48] T. Miao,[15] D. Mietlicki,[32] A. Mitra,[1] H. Miyake,[53] S. Moed,[20] N. Moggi,[6] M.N. Mondragon[k],[15] C.S. Moon,[25] R. Moore,[15] M.J. Morello,[15] J. Morlock,[24] P. Movilla Fernandez,[15] A. Mukherjee,[15] Th. Muller,[24] P. Murat,[15] M. Mussini[z],[6] J. Nachtman[m],[15] Y. Nagai,[53] J. Naganoma,[56] I. Nakano,[38] A. Napier,[54] J. Nett,[51] C. Neu,[55] M.S. Neubauer,[22] J. Nielsen[e],[26] L. Nodulman,[2] O. Norniella,[22] E. Nurse,[28] L. Oakes,[40] S.H. Oh,[14] Y.D. Oh,[25] I. Oksuzian,[55] T. Okusawa,[39] R. Orava,[21] L. Ortolan,[4] S. Pagan Griso[aa],[41] C. Pagliarone,[52] E. Palencia[f],[9] V. Papadimitriou,[15] A.A. Paramonov,[2] J. Patrick,[15] G. Pauletta[ff],[52] M. Paulini,[10] C. Paus,[30] D.E. Pellett,[7] A. Penzo,[52] T.J. Phillips,[14] G. Piacentino,[44] E. Pianori,[43] J. Pilot,[37] K. Pitts,[22] C. Plager,[8] L. Pondrom,[58] K. Potamianos,[46] O. Poukhov[*],[13] F. Prokoshin[x],[13] A. Pronko,[15] F. Ptohos[h],[17] E. Pueschel,[10] G. Punzi[bb],[44] J. Pursley,[58] A. Rahaman,[45] V. Ramakrishnan,[58] N. Ranjan,[46] I. Redondo,[29] P. Renton,[40] M. Rescigno,[49] F. Rimondi[z],[6] L. Ristori[45],[15] A. Robson,[19] T. Rodrigo,[9] T. Rodriguez,[43] E. Rogers,[22] S. Rolli,[54] R. Roser,[15] M. Rossi,[52] F. Rubbo,[15] F. Ruffini[cc],[44] A. Ruiz,[9] J. Russ,[10] V. Rusu,[15] A. Safonov,[51] W.K. Sakumoto,[47] Y. Sakurai,[56] L. Santi[ff],[52] L. Sartori,[44]

K. Sato,[53] V. Saveliev[t],[42] A. Savoy-Navarro,[42] P. Schlabach,[15] A. Schmidt,[24] E.E. Schmidt,[15] M.P. Schmidt[*],[59]
M. Schmitt,[36] T. Schwarz,[7] L. Scodellaro,[9] A. Scribano[cc],[44] F. Scuri,[44] A. Sedov,[46] S. Seidel,[35] Y. Seiya,[39]
A. Semenov,[13] F. Sforza[bb],[44] A. Sfyrla,[22] S.Z. Shalhout,[7] T. Shears,[27] P.F. Shepard,[45] M. Shimojima[s],[53]
S. Shiraishi,[11] M. Shochet,[11] I. Shreyber,[34] A. Simonenko,[13] P. Sinervo,[31] A. Sissakian[*],[13] K. Sliwa,[54] J.R. Smith,[7]
F.D. Snider,[15] A. Soha,[15] S. Somalwar,[50] V. Sorin,[4] P. Squillacioti,[15] M. Stancari,[15] M. Stanitzki,[59]
R. St. Denis,[19] B. Stelzer,[31] O. Stelzer-Chilton,[31] D. Stentz,[36] J. Strologas,[35] G.L. Strycker,[32] Y. Sudo,[53]
A. Sukhanov,[16] I. Suslov,[13] K. Takemasa,[53] Y. Takeuchi,[53] J. Tang,[11] M. Tecchio,[32] P.K. Teng,[1] J. Thom[g],[15]
J. Thome,[10] G.A. Thompson,[22] E. Thomson,[43] P. Ttito-Guzmán,[29] S. Tkaczyk,[15] D. Toback,[51] S. Tokar,[12]
K. Tollefson,[33] T. Tomura,[53] D. Tonelli,[15] S. Torre,[17] D. Torretta,[15] P. Totaro[ff],[52] M. Trovato[dd],[44] Y. Tu,[43]
F. Ukegawa,[53] S. Uozumi,[25] A. Varganov,[32] F. Vázquez[k],[16] G. Velev,[15] C. Vellidis,[3] M. Vidal,[29] I. Vila,[9]
R. Vilar,[9] J. Vizán,[60] M. Vogel,[35] G. Volpi[bb],[44] P. Wagner,[43] R.L. Wagner,[15] T. Wakisaka,[39] R. Wallny,[8]
S.M. Wang,[1] A. Warburton,[31] D. Waters,[28] M. Weinberger,[51] W.C. Wester III,[15] B. Whitehouse,[54] D. Whiteson[c],[43]
A.B. Wicklund,[2] E. Wicklund,[15] S. Wilbur,[11] F. Wick,[24] H.H. Williams,[43] J.S. Wilson,[37] P. Wilson,[15] B.L. Winer,[37]
P. Wittich[g],[15] S. Wolbers,[15] H. Wolfe,[37] T. Wright,[32] X. Wu,[18] Z. Wu,[5] K. Yamamoto,[39] J. Yamaoka,[14]
T. Yang,[15] U.K. Yang[p],[11] Y.C. Yang,[25] W.-M. Yao,[26] G.P. Yeh,[15] K. Yi[m],[15] J. Yoh,[15] K. Yorita,[56]
T. Yoshida[j],[39] G.B. Yu,[14] I. Yu,[25] S.S. Yu,[15] J.C. Yun,[15] A. Zanetti,[52] Y. Zeng,[14] and S. Zucchelli[z][6]

(CDF Collaboration[†])

[1]Institute of Physics, Academia Sinica, Taipei, Taiwan 11529, Republic of China
[2]Argonne National Laboratory, Argonne, Illinois 60439, USA
[3]University of Athens, 157 71 Athens, Greece
[4]Institut de Fisica d'Altes Energies, ICREA, Universitat Autonoma de Barcelona, E-08193, Bellaterra (Barcelona), Spain
[5]Baylor University, Waco, Texas 76798, USA
[6]Istituto Nazionale di Fisica Nucleare Bologna, [z]University of Bologna, I-40127 Bologna, Italy
[7]University of California, Davis, Davis, California 95616, USA
[8]University of California, Los Angeles, Los Angeles, California 90024, USA
[9]Instituto de Fisica de Cantabria, CSIC-University of Cantabria, 39005 Santander, Spain
[10]Carnegie Mellon University, Pittsburgh, Pennsylvania 15213, USA
[11]Enrico Fermi Institute, University of Chicago, Chicago, Illinois 60637, USA
[12]Comenius University, 842 48 Bratislava, Slovakia; Institute of Experimental Physics, 040 01 Kosice, Slovakia
[13]Joint Institute for Nuclear Research, RU-141980 Dubna, Russia
[14]Duke University, Durham, North Carolina 27708, USA
[15]Fermi National Accelerator Laboratory, Batavia, Illinois 60510, USA
[16]University of Florida, Gainesville, Florida 32611, USA
[17]Laboratori Nazionali di Frascati, Istituto Nazionale di Fisica Nucleare, I-00044 Frascati, Italy
[18]University of Geneva, CH-1211 Geneva 4, Switzerland
[19]Glasgow University, Glasgow G12 8QQ, United Kingdom
[20]Harvard University, Cambridge, Massachusetts 02138, USA
[21]Division of High Energy Physics, Department of Physics,
University of Helsinki and Helsinki Institute of Physics, FIN-00014, Helsinki, Finland
[22]University of Illinois, Urbana, Illinois 61801, USA
[23]The Johns Hopkins University, Baltimore, Maryland 21218, USA
[24]Institut für Experimentelle Kernphysik, Karlsruhe Institute of Technology, D-76131 Karlsruhe, Germany
[25]Center for High Energy Physics: Kyungpook National University,
Daegu 702-701, Korea; Seoul National University, Seoul 151-742,
Korea; Sungkyunkwan University, Suwon 440-746,
Korea; Korea Institute of Science and Technology Information,
Daejeon 305-806, Korea; Chonnam National University, Gwangju 500-757,
Korea; Chonbuk National University, Jeonju 561-756, Korea
[26]Ernest Orlando Lawrence Berkeley National Laboratory, Berkeley, California 94720, USA
[27]University of Liverpool, Liverpool L69 7ZE, United Kingdom
[28]University College London, London WC1E 6BT, United Kingdom
[29]Centro de Investigaciones Energeticas Medioambientales y Tecnologicas, E-28040 Madrid, Spain
[30]Massachusetts Institute of Technology, Cambridge, Massachusetts 02139, USA
[31]Institute of Particle Physics: McGill University, Montréal, Québec,
Canada H3A 2T8; Simon Fraser University, Burnaby, British Columbia,
Canada V5A 1S6; University of Toronto, Toronto, Ontario,
Canada M5S 1A7; and TRIUMF, Vancouver, British Columbia, Canada V6T 2A3
[32]University of Michigan, Ann Arbor, Michigan 48109, USA
[33]Michigan State University, East Lansing, Michigan 48824, USA
[34]Institution for Theoretical and Experimental Physics, ITEP, Moscow 117259, Russia

[35]University of New Mexico, Albuquerque, New Mexico 87131, USA

[36]Northwestern University, Evanston, Illinois 60208, USA

[37]The Ohio State University, Columbus, Ohio 43210, USA

[38]Okayama University, Okayama 700-8530, Japan

[39]Osaka City University, Osaka 588, Japan

[40]University of Oxford, Oxford OX1 3RH, United Kingdom

[41]Istituto Nazionale di Fisica Nucleare, Sezione di Padova-Trento, [aa]University of Padova, I-35131 Padova, Italy

[42]LPNHE, Universite Pierre et Marie Curie/IN2P3-CNRS, UMR7585, Paris, F-75252 France

[43]University of Pennsylvania, Philadelphia, Pennsylvania 19104, USA

[44]Istituto Nazionale di Fisica Nucleare Pisa, [bb]University of Pisa,

[cc]University of Siena and [dd]Scuola Normale Superiore, I-56127 Pisa, Italy

[45]University of Pittsburgh, Pittsburgh, Pennsylvania 15260, USA

[46]Purdue University, West Lafayette, Indiana 47907, USA

[47]University of Rochester, Rochester, New York 14627, USA

[48]The Rockefeller University, New York, New York 10065, USA

[49]Istituto Nazionale di Fisica Nucleare, Sezione di Roma 1,

[ee]Sapienza Università di Roma, I-00185 Roma, Italy

[50]Rutgers University, Piscataway, New Jersey 08855, USA

[51]Texas A&M University, College Station, Texas 77843, USA

[52]Istituto Nazionale di Fisica Nucleare Trieste/Udine,

I-34100 Trieste, [ff]University of Trieste/Udine, I-33100 Udine, Italy

[53]University of Tsukuba, Tsukuba, Ibaraki 305, Japan

[54]Tufts University, Medford, Massachusetts 02155, USA

[55]University of Virginia, Charlottesville, VA 22906, USA

[56]Waseda University, Tokyo 169, Japan

[57]Wayne State University, Detroit, Michigan 48201, USA

[58]University of Wisconsin, Madison, Wisconsin 53706, USA

[59]Yale University, New Haven, Connecticut 06520, USA

[60]Instituto de Fisica de Cantabria, CSIS-University of Cantabria, 39005 Santander, Spain

We present a measurement of the top quark mass in the lepton+jets and dilepton channels of $t\bar{t}$ decays using the template method. The data sample corresponds to an integrated luminosity of 5.6 fb^{-1} of $p\bar{p}$ collisions at Tevatron with $\sqrt{s} = 1.96$ TeV, collected with the CDF II detector. The measurement is performed by constructing templates of three kinematic variables in the lepton+jets and two kinematic variables in the dilepton channel. The variables are two reconstructed top quark masses from different jets-to-quarks combinations and the invariant mass of two jets from the W decay in the lepton+jets channel, and a reconstructed top quark mass and m_{T2}, a variable related to the transverse mass in events with two missing particles, in the dilepton channel. The simultaneous fit of the templates from signal and background events in the lepton+jets and dilepton channels to the data yields a measured top quark mass of $M_{top} = 172.1 \pm 1.1$ (stat) ± 0.9 (syst) GeV/c^2.

*Deceased

†With visitors from [a]University of Massachusetts Amherst, Amherst, Massachusetts 01003, [b]Istituto Nazionale di Fisica Nucleare, Sezione di Cagliari, 09042 Monserrato (Cagliari), Italy, [c]University of California Irvine, Irvine, CA 92697, [d]University of California Santa Barbara, Santa Barbara, CA 93106 [e]University of California Santa Cruz, Santa Cruz, CA 95064, [f]CERN,CH-1211 Geneva, Switzerland, [g]Cornell University, Ithaca, NY 14853, [h]University of Cyprus, Nicosia CY-1678, Cyprus, [i]University College Dublin, Dublin 4, Ireland, [j]University of Fukui, Fukui City, Fukui Prefecture, Japan 910-0017, [k]Universidad Iberoamericana, Mexico D.F., Mexico, [l]Iowa State University, Ames, IA 50011, [m]University of Iowa, Iowa City, IA 52242, [n]Kinki University, Higashi-Osaka City, Japan 577-8502, [o]Kansas State University, Manhattan, KS 66506, [p]University of Manchester, Manchester M13 9PL, England, [q]Queen Mary, University of London, London, E1 4NS, England, [r]Muons, Inc., Batavia, IL 60510, [s]Nagasaki Institute of Applied Science, Nagasaki, Japan, [t]National Research

The top quark (t) is by far the heaviest known elementary particle [1]. The top quark contributes significantly to electroweak radiative corrections relating the top quark mass (M_{top}) and the W boson mass to the mass of the predicted Higgs boson [2, 3]. Precision measurements of M_{top} provide therefore important constraints on the Higgs boson mass. Since the discovery of the top quark in 1995 [4] at the Fermilab Tevatron $p\bar{p}$ Collider, both the CDF and D0 experiments have been improving the precision of the M_{top} measurement [5]. However it

Nuclear University, Moscow, Russia, [u]University of Notre Dame, Notre Dame, IN 46556, [v]Universidad de Oviedo, E-33007 Oviedo, Spain, [w]Texas Tech University, Lubbock, TX 79609, [x]Universidad Tecnica Federico Santa Maria, 110v Valparaiso, Chile, [y]Yarmouk University, Irbid 211-63, Jordan, [gg]On leave from J. Stefan Institute, Ljubljana, Slovenia,

is important to measure M_{top} using different techniques and independent data samples in different decay channels. Significant differences in the measurements of M_{top} in different decay channels could indicate contributions from new physics beyond the SM [6].

This letter reports a measurement of the top quark mass using the template method [7–9]. We use samples of $t\bar{t}$ candidates in the lepton+jets and dilepton channels, corresponding to an integrated luminosity of 5.6 fb^{-1} of proton-antiproton collisions at $\sqrt{s} = 1.96$ TeV, collected by the CDF II detector [10]. This is a general-purpose detector designed to study $p\bar{p}$ collisions at the Fermilab Tevatron. A charged-particle tracking system, consisting of a silicon microstrip tracker and a drift chamber, is immersed in a 1.4 T magnetic field. Electromagnetic and hadronic calorimeters surround the tracking system and measure particle energies. Drift chambers and scintillators, located outside the calorimeters, detect muon candidates.

Assuming unitarity of the three-generation CKM matrix, the top quark decays almost exclusively into a W boson and a b quark [1]. The case where one W decays leptonically into an electron or a muon plus a neutrino and the other hadronically into a pair of jets defines the lepton+jets decay channel. The dilepton channel is defined as the case where both W's decay leptonically into an electron or a muon plus a neutrino.

Lepton+jets events are selected by requiring one isolated [11] electron (muon) with $E_T > 20$ GeV ($p_T > 20$ GeV/c) and pseudorapidity $|\eta| < 1.1$ [12]. We also require high missing transverse energy [13], $\not{E}_T > 20$ GeV, and at least four jets. Jets are reconstructed with a cone algorithm [14] with radius $R = \sqrt{(\Delta\eta)^2 + (\Delta\phi)^2} = 0.4$. Jets originating from b quarks are identified (tagged) using a secondary vertex tagging algorithm [15]. We request at least one jet to be tagged as a b jet. We divide the sample of candidate lepton+jets events into sub-samples of one b-tagged jet (1-tag) and two or more b-tagged jets (2-tag). In events with more than two b-tagged jets, we consider the two highest E_T jets as b quark candidates and treat the other b-tagged jets as non b-tagged jets. In the 1-tag sample, we require exactly four jets with transverse energy $E_T > 20$ GeV and $|\eta| < 2.0$. In the 2-tag sample, three jets are required to have $E_T > 20$ GeV and $|\eta| < 2.0$, and at least one more jet is required to have $E_T > 12$ GeV and $|\eta| < 2.4$. We apply an additional cut on the scalar sum of transverse energies in the event, $H_T = E_T^{\text{lepton}} + \not{E}_T + \sum_{jets} E_T^{\text{jet}}$, requiring $H_T > 250$ GeV for all events to further reject backgrounds. $E_T^{\text{muon}} = p_T^{\text{muon}}$ is assumed in the H_T calculation.

The primary sources of background in the lepton+jets channel are W+jets and QCD multijet production. We also consider small contributions from Z+jets, diboson, and single-top production. To estimate the contribution of each process, we use a combination of data and Monte Carlo (MC) based techniques described in Ref. [16]. For the Z+jets, diboson, single top, and $t\bar{t}$ events we nor-

TABLE I: Expected and observed numbers of signal and background events assuming $t\bar{t}$ production cross section $\sigma_{t\bar{t}} = 7.4$ pb and $M_{top} = 172.5$ GeV/c^2 in the lepton+jets channel.

	1-tag	2-tag
W+jets	53.4 ± 17.5	8.5 ± 3.0
QCD multijet	13.1 ± 10.6	1.8 ± 1.5
Z+jets	4.7 ± 1.0	0.5 ± 0.1
Diboson	6.3 ± 0.8	0.8 ± 0.1
Single top	4.9 ± 0.4	2.0 ± 0.2
Background	105 ± 21	14.2 ± 3.3
$t\bar{t}$ signal	590 ± 74	293 ± 45
Expected	694 ± 77	307 ± 45
Observed	695	286

malize MC simulation events using their respective theoretical cross sections [17–19]. QCD multijet background is estimated using the data referring to techniques described in Ref. [20]. The shape of W+jets background is obtained from MC while the number of W+jets events is determined from the data by subtracting all the other backgrounds and $t\bar{t}$.

Three observables are used from each lepton+jets event: two reconstructed top quark masses (m_t^{reco} and $m_t^{\text{reco}(2)}$) and the invariant mass of the two jets from the hadronically decaying W boson (m_{jj}). We have complete reconstruction of the $t\bar{t}$ kinematics in the lepton+jets channel [7, 8] with constraints from the precise W boson mass and requiring the t and $\bar{t}$ masses to be the same. With the assumption that the leading four jets in the detector come from the $t\bar{t}$ decay products, there are six and two possible assignments of jets to quarks for 1-tag and 2-tag respectively. A minimization is performed for each assignment using a χ^2 comparison to the $t\bar{t}$ hypothesis with m_t^{reco} taken from the assignment that yields the lowest χ^2. To increase the statistical power of the measurement, we employ an additional observable $m_t^{\text{reco}(2)}$ from the assignment that yields the 2nd lowest χ^2. Events with the lowest $\chi^2 > 9.0$ are removed from the sample to reject poorly reconstructed events. The dijet mass m_{jj} is calculated as the invariant mass of two non b-tagged jets which provides the closest value to the world average W boson mass of 80.40 GeV/c^2 [1]. We apply boundary cuts on m_t^{reco} and $m_t^{\text{reco}(2)}$ (100 GeV/$c^2 < m_t^{\text{reco}}, m_t^{\text{reco}(2)} < 350$ GeV/c^2) and m_{jj} (50 GeV/$c^2 < m_{jj} < 120$ GeV/c^2 for 1-tag events and 50 GeV/$c^2 < m_{jj} < 125$ GeV/c^2 for 2-tag events), and normalize the probability density function in the signal region. The estimated number of background events and the observed number of events after event selection, χ^2 cut, and boundary cuts are listed in Table I for the lepton+jets decay channel.

To select dilepton candidate events, we require two oppositely charged leptons with $E_T > 20$ GeV (for electrons) or $p_T > 20$ GeV/c (for muons). One lepton is

TABLE II: Expected and observed number of signal and background events assuming $t\bar{t}$ production cross section $\sigma_{t\bar{t}} = 7.4$ pb and $M_{top} = 172.5$ GeV/c^2 in the dilepton channel.

	non-tagged	tagged
Diboson	19.2 ± 3.3	0.7 ± 0.2
Drell-Yan	31.5 ± 3.9	3.7 ± 0.2
W+jets (fake lepton)	30.8 ± 9.4	4.6 ± 1.3
Background	81.6 ± 10.4	8.9 ± 1.4
$t\bar{t}$ signal	124 ± 16	151 ± 19
Expected	205 ± 19	160 ± 19
Observed	237	155

required to be isolated in the central region ($|\eta| < 1.1$) of the detector, but the other can be a non-isolated lepton in the central region or an isolated electron in the forward region ($1.1 < |\eta| < 2.0$). We also require $\not{E}_T > 25$ GeV, and at least two jets with $E_T > 15$ GeV and $|\eta| < 2.5$. To further reject backgrounds, we require $H_T > 200$ GeV. In measuring the top quark mass, we divide the dilepton sample into events with b-tagged jets (tagged) and without b-tagged jets (non-tagged).

Drell-Yan, diboson, and W+jets (fake lepton) events are the primary sources of background in the dilepton channel. We estimate the rate of the Drell-Yan and diboson events with calculations based on MC simulations. For the Drell-Yan Z+jets process, we normalize the MC sample by matching the number of Z events predicted and observed in the Z mass region between 76 GeV/c^2 and 106 GeV/c^2. We use data to estimate the rate of W+jets (fake lepton) events where an event has one real lepton and one of the jets misidentified as the other lepton. The detailed procedure of background estimation in the dilepton channel is described in Ref. [21]. For each event we calculate a reconstructed top quark mass m_t^{NWA} using the neutrino weighting algorithm [22], and we calculate a quantity m_{T2} [23]. Here m_{T2} is a variable related to the transverse mass of the mother particles (top quark in the $t\bar{t}$ system) in events with two missing particles from pair production of the mother particles. We firstly use this variable for the top quark mass measurement in the dilepton channel [9]. We require these observables to be consistent with the top quark signal by demanding 100 GeV/$c^2 < m_t^{NWA} < 350$ GeV/c^2 and 30 GeV/$c^2 < m_{T2} < 200$ GeV/c^2. The estimated number of background events and the observed number of events after event selection are listed in Table II for the dilepton decay channel.

We estimate the probability density functions (p.d.f.'s) of signal and background using kernel density estimation (KDE) [24]. In the lepton+jets channel, we use the three dimensional KDE that accounts for the correlation between the three observables. In the dilepton channel, instead, we use the two dimensional KDE. The dijet mass m_{jj} of the two jets assigned to the W in the lepton+jets channel is used for in $situ$ calibration of jet energy scale (JES) [7, 8]. The p.d.f.'s for the observables

are estimated at discrete values of M_{top} from 130 GeV/c^2 to 220 GeV/c^2, with increments from 0.5 GeV/c^2 in the region immediately above and below 172.5 GeV/c^2 to 5 GeV/c^2 near the extreme mass values, and at discrete values of Δ_{JES} from -3.0 σ_c to 3.0 σ_c with increments of 0.2 σ_c, where σ_c is the CDF JES fractional uncertainty [25] and Δ_{JES} corresponds to the difference between the energy scale in MC simulation and data. We interpolate the MC distributions to find p.d.f.'s for arbitrary values of M_{top} and Δ_{JES} using the local polynomial smoothing method [26]. We fit the signal and background p.d.f.'s to the distributions of the observables in the data using an unbinned maximum likelihood fit [27] where we minimize the negative logarithm of the likelihood using MINUIT [28]. The likelihood is built for each sub-sample separately, 1-tag and 2-tag for lepton+jets events, non-tagged and tagged for dilepton events, and an overall likelihood is then obtained by multiplying them together. We independently obtain the results from the lepton+jets channel, the dilepton channel, and the two channels combined. In the combined fit, the dilepton channel uses the JES calibration found in the lepton+jets channel. We evaluate the statistical uncertainty on M_{top} by searching for the points where the negative logarithm of the likelihood exeeds the minimum by 0.5. Ref. [8, 9] provides detailed information about this technique.

We test the mass fit procedures using 3000 pseudoexperiments for a set of 14 different M_{top} values ranging from 159 GeV/c^2 to 185 GeV/c^2. In each experiment, we select the number of background events from a Poisson distribution with a mean equal to the expected total number of background events in the sample and the number of signal events from a Poisson distribution with a mean equal to the expected number of signal events normalized to a $t\bar{t}$ pair production cross section of 7.4 pb at $M_{top} = 172.5$ GeV/c^2 [19]. The distributions of the average mass residual (deviation from the input top mass) and the width of the pull (the ratio of the residual to the uncertainty reported by MINUIT) for simulated experiments are corrected to be unity and zero respectively. The corrections are $m_{corr} = 1.04 \times m_{meas} - 6.8$ GeV/c^2, $m_{corr} = 1.03 \times m_{meas} - 5.5$ GeV/c^2, and $m_{corr} = 1.03 \times m_{meas} - 5.9$ GeV/c^2 for combined fit, lepton+jets, and dilepton channel respectively, where m_{meas} is the raw value from likelihood fit and m_{corr} is the corrected value of the measurement. We increase the measured uncertainty by 4% for combined fit and lepton+jets channel and 3% for dilepton channel to correct the width of the pull.

We examine various sources of systematic uncertainties that could affect the measurement by comparing the results of pseudoexperiments in which we vary relevant parameters within their systematic uncertainties. The dominant sources of systematic uncertainty are the residual JES [8, 25] and signal modeling. We vary JES parameters within their uncertainties in both signal and background MC generated events and interpret the shifts in the results of the pseudoexperiments as uncertainties. For the
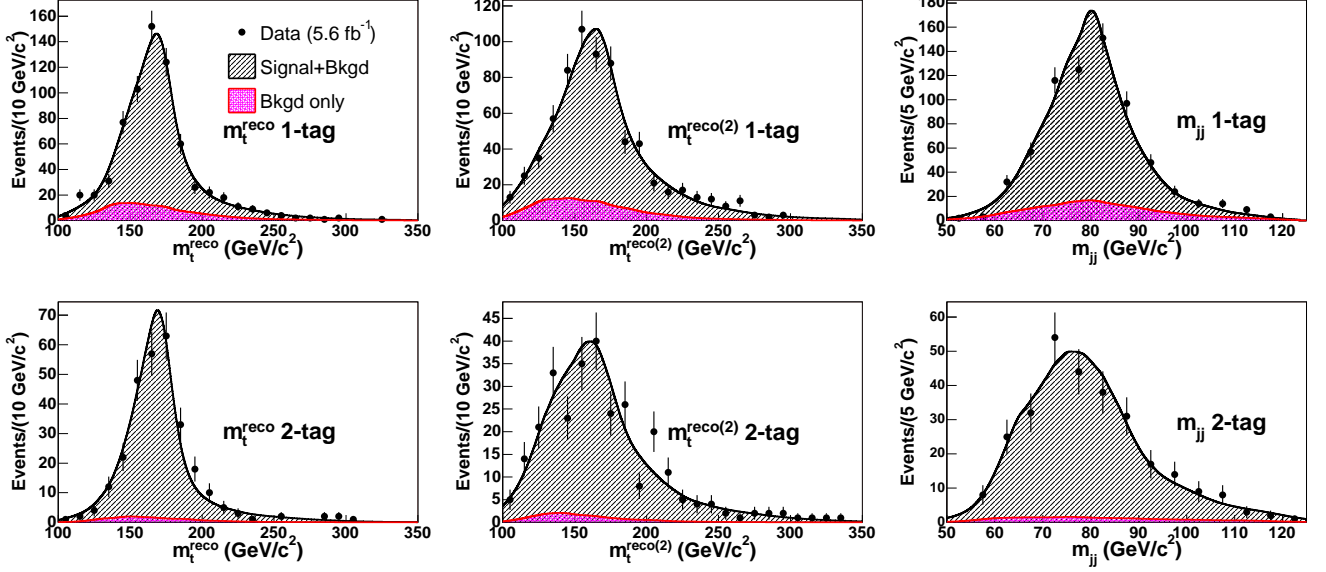
FIG. 1: Distributions of the three variables used to measure M_{top} in the lepton+jets channel, showing 1-tag and 2-tag samples separately. The data are overlaid with the predictions from the KDE probability distributions using $M_{top} = 172.0$ GeV/c^2 and the full background model.
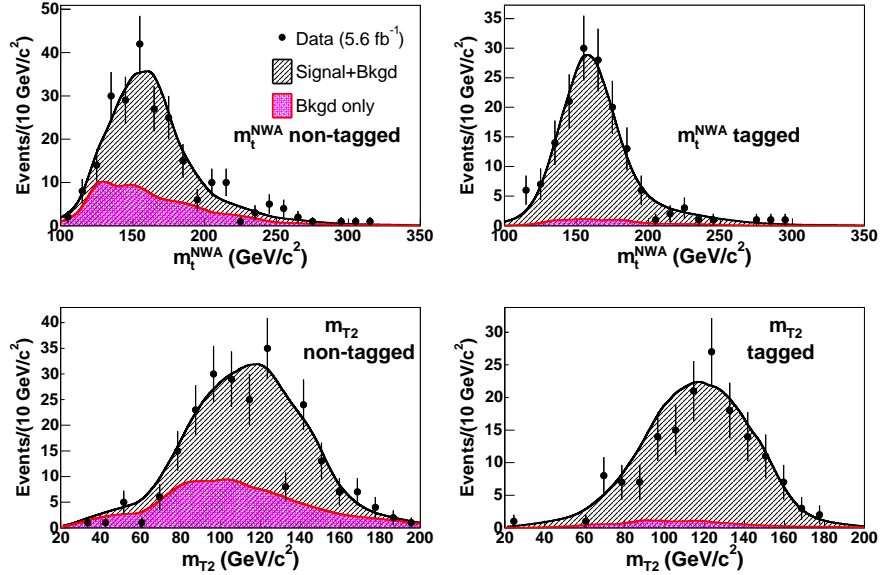

FIG. 2: Distributions of the two variables used to measure M_{top} in the dilepton channel, showing non-tagged and tagged samples separately. The data are overlaid with the predictions from the KDE probability distributions using $M_{top} = 170.0$ GeV/c^2 and the full background model.

dilepton channel, which has no *in situ* calibration, the JES is the single dominant uncertainty. The uncertainty arising from the choice of MC generator (signal modeling) is estimated by comparing the results of pseudoexperiments generated with PYTHIA [29] and HERWIG [30]. The b-JES systematic uncertainty arising from our modeling of b fragmentation, b hadron branching fractions, and calorimeter response captures the additional uncer-

tainty not taken into account in the (residual) JES. We estimate the systematic uncertainty due to modeling of initial-state gluon radiation and final-state gluon radiation by extrapolating uncertainties in the p_T of Drell-Yan events to the $t\bar{t}$ mass region [7]. We vary the parameters of parton distribution functions (PDFs) and gluon fusion fraction within their uncertainties to account systematic effects. We estimate systematic uncertainties due

TABLE III: Estimated systematic uncertainties in the combined fit (Comb), lepton+jets (LJ), and dilepton (DIL) (unit in GeV/c^2).

Source	Comb	LJ	DIL
(Residual) Jet Energy Scale	0.5	0.5	3.0
Signal modeling	0.7	0.7	0.3
b Jet energy scale	0.3	0.3	0.4
Initial and final state radiation	0.1	0.1	0.2
Parton distribution functions	0.1	0.1	0.3
Gluon fusion fraction	<0.1	<0.1	0.1
Lepton energy	<0.1	0.1	0.3
Background shape	0.1	0.1	0.3
Multiple hadron interaction	0.2	0.1	0.2
Color reconnection	0.2	0.2	0.5
MC statistics	0.1	0.1	0.1
Total systematic uncertainty	0.9	0.9	3.1

to the lepton energy and momentum scales by propagating shifts in electron energy and muon momentum scales within their uncertainties. Background shape systematic uncertainties account for the variation of the background composition. We estimate the multiple hadron interaction systematic uncertainty to account the effect from the difference in the average number of interactions between MC samples and the data. The color reconnection (CR) systematic uncertainty [31] is evaluated by MC samples generated with and without CR effects using different tunes [32] of PYTHIA. The total systematic uncertainties, adding individual components in quadrature, are 0.9 GeV/c^2 in the combined fit, 0.9 GeV/c^2 in the lepton+jets channel, and 3.1 GeV/c^2 in the dilepton channel.

We perform the likelihood fits to the data using the observables discussed in this letter and apply the corrections obtained using the simulated experiments. We obtain for the lepton+jets channel, a top quark mass

$$
\begin{aligned}
\mathrm{M_{top}} &= 172.2 \pm 1.2 \text{ (stat)} \pm 0.9 \text{ (syst) GeV}/c^2 \\
&= 172.2 \pm 1.5 \text{ GeV}/c^2,
\end{aligned}
$$

while for the dilepton channel,

$$
\begin{aligned}
\mathrm{M_{top}} &= 170.3 \pm 2.0 \text{ (stat)} \pm 3.1 \text{ (syst) GeV}/c^2 \\
&= 170.3 \pm 3.7 \text{ GeV}/c^2.
\end{aligned}
$$

The two channel combined fit yields a top quark mass

$$
\begin{aligned}
\mathrm{M_{top}} &= 172.1 \pm 1.1 \text{ (stat)} \pm 0.9 \text{ (syst) GeV}/c^2 \\
&= 172.1 \pm 1.4 \text{ GeV}/c^2.
\end{aligned}
$$

Figure 1 shows the measured distributions of the observables used for the $\mathrm{M_{top}}$ measurement in the lepton+jets channel overlaid with density estimates using $t\bar{t}$ signal events with $\mathrm{M_{top}} = 172$ GeV/c^2 (close to the measured $\mathrm{M_{top}}$ in the lepton+jets channel) and the full background model. Figure 2 shows the corresponding distributions in the dilepton channel using $t\bar{t}$ signal events with $\mathrm{M_{top}} = 170$ GeV/c^2 (close to the measured $\mathrm{M_{top}}$ in the dilepton channel).

In conclusion, we have performed a measurement of the top quark mass using the template method simultaneously in the lepton+jets and dilepton channels. The result, $\mathrm{M_{top}} = 172.1 \pm 1.4$ GeV/c^2, is consistent with the most recent world average of $\mathrm{M_{top}} = 173.3 \pm 1.1$ GeV/c^2 [5]. In the lepton+jets channel, we use the same data set as the best single $\mathrm{M_{top}}$ measurement [33], and have a consistent result with slightly larger uncertainty. In the dilepton channel, we achieve the single most precise measurement of $\mathrm{M_{top}}$ in this channel to date and the result is in good agreement with the measurement in the lepton+jets channel.

[1] C. Amsler *et al.* (Particle Data Group), Phys. Lett. B **667**, 1 (2008).
[2] ALEPH, CDF, D0, DELPHI, L3, OPAL, SLD, the LEP Electroweak Working Group, the Tevatron Electroweak Working Group, and the SLD Electroweak and Heavy Flavor Working Groups, arXiv:1012.2367v2.

[3] H. Flächer *et al.*, Eur. Phys. J. C **60**, 543 (2009).

[4] F. Abe *et al.* (CDF Collaboration), Phys. Rev. Lett. **74**, 2626 (1995); S. Abachi *et al.* (D0 Collaboration), Phys. Rev. Lett. **74**, 2632 (1995).

[5] The Tevatron Electroweak Working Group (CDF and D0 Collaborations), FERMILAB-TM-2466-E, arXiv:1007.3178v1.

[6] G. L. Kane and S. Mrenna, Phys. Rev. Lett. **77**, 3502 (1996).

[7] A. Abulencia *et al.* (CDF Collaboration), Phys. Rev. D **73**, 032003 (2006).

[8] T. Aaltonen *et al.* (CDF Collaboration), Phys. Rev. D **79**, 092005 (2009).

[9] T. Aaltonen *et al.* (CDF Collaboration), Phys. Rev. D **81**, 031102 (2010).

[10] D. Acosta *et al.* (CDF Collaboration), Phys. Rev. D **71**, 032001 (2005).

[11] A lepton is isolated when $\left(p_T^{\mathrm{total}} - p_T^{\mathrm{lepton}}\right)/p_T^{\mathrm{lepton}} <$ 0.1, where p_T^{total} is the total transverse momentum (energy) and p_T^{lepton} is the lepton transverse momentum (energy) for muon (electron) in a cone of radius $\Delta R \equiv \sqrt{(\Delta\eta)^2 + (\Delta\phi)^2} = 0.4$ [12] with axis along the direction of the lepton.

[12] We use a right-handed spherical coordinate system with the origin at the center of the detector with the z-axis along the proton beam and the y-axis poiting up. θ and ϕ are the polar and azimuthal angles, respectively. The pseudorapidity is defined by $\eta = -\ln\tan(\theta/2)$. The transverse momentum and energy of a detected particle or jet are defined by $p_T = p\sin(\theta)$ and $E_T = E\sin(\theta)$, respectively, where p and E are the momentum and energy of the particle. For the reconstructed top quark decay products used in the m_{T2} calculation, the transverse energy is defined by $E_T = \sqrt{m^2 + p_T^2}$, where m is the mass of the product.

[13] The missing transverse energy, an imbalance of energy in the transverse plane of the detector, is defined by $\not{E}_T = |\sum_{towers} E_T \hat{n}_T|$, where $\hat{n}_T$ is the unit vector normal to the beam and pointing to a given calorimeter tower and E_T is the transverse energy measured in that tower.

[14] F. Abe *et al.* (CDF Collaboration), Phys. Rev. D **45**, 1448 (1992).

[15] D. Acosta *et al.* (CDF Collaboration), Phys. Rev. D **71**, 052003 (2005).

[16] T. Aaltonen *et al.* (CDF Collaboration), Phys. Rev. Lett. **105**, 012001 (2010).

[17] J. M. Campbell and R. K. Ellis, Phys. Rev. D **60**, 113006 (1999).

[18] B. W. Harris *el al.*, Phys. Rev. D **66**, 054024 (2002).

[19] S. Moch and P. Uwer, Nucl. Phys. B, Proc. Suppl. **183**, 75 (2008).

[20] T. Aaltonen *el al.* (CDF Collaboration), Phys. Rev. D **77**, 011108 (2008).

[21] T. Aaltonen *et al.* (CDF Collaboration), Phys. Rev. D **82**, 052002 (2010).

[22] B. Abbott *et al.* (D0 Collaboration), Phys. Rev. D **60**, 052001 (1999); A. Abulencia *et al.*, Phys. Rev. D **73**, 112006 (2006).

[23] C. Lester and D. Summers, Phys. Lett. B **463**, 99 (1999); A. Barr, C. Lester, and P. Stephens, J. Phys. G **29**, 2343 (2003).

[24] K. Cranmer, Comput. Phys. Commun. **136** 198 (2001).

[25] A. Bhatti *et al.*, Nucl. Instrum. Methods Phys. Res. Sect. A **566** 375 (2006).

[26] C. Loader, *Local Regression and Likelihood* (Springer, New York, 1999).

[27] R. Barlow, Nucl. Instrum. Methods Phys. Res. Sect. A **297** 496 (1990).

[28] F. James and M. Roos, Comput. Phys. Commun. **10** 343 (1975).

[29] T. Sjöstrand, S. Mrenna, and P. Skands, J. High Energy Phys. 05 (2006) 026.

[30] G. Corcella *et al.*, J. High Energy Phys. 01 (2001) 010.

[31] P. Z. Skands and D. Wicke, Eur. Phys. J. C **52**, 133 (2007).

[32] P. Z. Skands, Phys. Rev. D **82**, 074018 (2010).

[33] T. Aaltonen *et al.* (CDF Collaboration), Phys. Rev. Lett. **105**, 252001 (2010).